Hygrothermal performance of an internally insulated masonry wall: Experimentations without a vapour barrier in a historic Italian Palazzo

Mirco Andreotti [a], Marta Calzolari [b], Pietromaria Davoli [b], Luísa Dias Pereira [b,1,*]

[a] *Istituto Nazionale di Fisica Nucleare, Sezione di Ferrara, via Saragat 1, 44122 Ferrara, Italy*
[b] *Architettura>Energia Research Centre, Department of Architecture, University of Ferrara, via Ghiara 36, 44121 Ferrara, Italy*

ABSTRACT

This paper presents the newly developed study, methodology and assessment of the hygrothermal performance of a historic building wall retrofitted with three different internal insulation technologies, without a vapour barrier. It aims at assessing any possible condensation problems at the most critical point of the tested stratigraphy (namely, in between the wall and the insulation material) and to limit the modification of the original hygrothermal behaviour of the original wall's materials with the addition of a vapour layer, as would commonly be used. This evaluation was performed through in situ measurements and dynamic software simulations. In situ data was used for calibrating the 2D simulation model conducted with Delphin software 6.0.20.

Under the climatic conditions in Ferrara (Italy), the results of both the in-situ monitoring and simulation evidenced no risk of frost damage to the building's original wall. With regards to the risk of interstitial condensation, simulations showed no high risk even in the absence of a water vapour barrier. Additionally, the amount of water vapour collected during the winter season dried out during the spring/summer period.

1. Introduction

Energy consumption of buildings is still a subject currently under the spotlight, as buildings are major consumers of energy [1]. At a European level, since 2012 (through the European Directive 2012/27/UE [2]), it has been suggested that there is a need to establish plans for energy efficiency in buildings, as a valuable means in addressing the challenges related to the scarcity of energy resources, climate change and the economic crisis. Even with the encouragement of such policies, the existing European building stock still requires vital and prompt actions. The recognition of this fact has recently been (re)acknowledged: the Directive amending the Energy Performance of Buildings Directive (2018/844/EU) [3] and the Renovation wave [4] of public and private buildings, as part of the European Green Deal [5], are two important strategies with the same mission – improvement of the energy efficiency of the EU building stock. Within this frame-

work, historic heritage has to be involved in terms of the maintenance of its architectural, in its social and in its historical values for the next generations.

Heritage values are naturally protected by several international institutions and codes [6], as the United Nations Educational, Scientific and Cultural Organization (UNESCO) [7], environmental sustainability certification schemes [8], or by national legislations, for example the D.L. 22 gennaio 2004, n. 42 Codice dei beni culturali e del paesaggio, in Italy [9] or the Swedish Planning and Building Act (SFS), [10] cited in [11]. The energy enhancement path of historic buildings (HB) deserves the same attention. Even if it is still under development, this practice is increasing, as demonstrated by several new guidelines and regulations, for example: i) the *Guidelines for energy efficiency in cultural heritage. Architecture, historic and urban centers and nuclei* in Italy [12]; ii) the EN 16883:2017 – Guidelines for improving the energy performance of historic buildings [13]; or iii) the recently released report by ICOMOS – Future of Our Pasts: Engaging Cultural Heritage in Climate Action [14].

Among the various critical issues and barriers related to the renovation processes of HB, the improvement of the envelope energy performance in compliance with the historic values, is one of the most delicate aspects. It is particularly difficult when

* Corresponding author.

E-mail addresses: mirco.andreotti@fe.infn.it (M. Andreotti), marta.calzolari@unife.it (M. Calzolari), pietromaria.davoli@unife.it (P. Davoli), dsplmr@unife.it (L. Dias Pereira).

[1] Department of Mechanical Engineering Pólo II, University of Coimbra, ADAI-LAETA, Rua Luís Reis Santos, 3030-788 Coimbra, Portugal;

working on the vertical opaque surfaces (historic walls), due to the simple reading of each intervention and due to the potential interference of such interventions with the original hygrothermal behaviour of the historic masonry.

In protected or listed HBs, adding an internal insulation layer (when in the absence of decorations) is often the only possible retrofit wall solution. Nonetheless, contrary to the external insulation, this solution presents several disadvantages [15] an example: losing inner space when adding the layer of insulation [16]; adding an internal insulation layer to an existing wall means that the temperature level of the wall will be lowered and therefore the drying capacity of the wall will be reduced, leading to higher moisture levels on the inner face of the wall and eventually generating interstitial condensation [17].

When the implementation of energy-efficiency measures places risks of destruction to the heritage values, a case-by-case analysis of the possible solutions should be made. For this reason, such choices have been the objective of several studies: (i) Hansen et al. conducted their study in Denmark testing four historic building façades retrofitted with internal insulation [18]; (ii) Hamid and Wallentén focused on Swedish multifamily buildings [19]; (iii) Kloseiko, Arumagi and Kalamees ran a similar study in a school building in Estonia [20]; (iv) while Walker and Pavia performed their study on the walls of the Adjutant General's Building of the Royal Hospital Kilmainham, in Dublin [21].

Within this context, the most intuitive and common solution, considering the current insulation technologies on the market, would be adding a water vapour barrier to the insulation layer, minimizing the impacts of the internally generated vapour transported through the retrofitted wall. Nevertheless, this option brings several criticalities: (i) tightening the indoor environment likely leads to 'increased demands of ventilation to preserve hygrothermal comfort inside the building' [15] (p.52), delaying the phenomena of vapour transport but only up to a certain extent; (ii) 'water vapour barriers are very sensitive to mechanical damage' [15] (p.52) – its effect can be immediately compromised, for example in the presence of plugs or when users decide to nail something to the wall or to hang something, therefore limiting the use of the wall; (iii) it significantly changes the 'traditional' water vapour diffusion transportation characteristics of historic brick walls (water vapour diffusion resistance (μ) of "historic bricks" range 6.8–168, Delphin Material Database [22]; "clay bricks" μ value 15 – 67 range in [23]). For all these reasons, most of the time, national conservation authorities judge the addition of an impermeable layer as an unacceptable alteration of the original hygrothermal behaviour of the historic envelope, therefore freezing or stopping the entire intervention.

Under this framework, authors have developed HeLLo - Heritage energy Living Lab onsite [24], a MSCA-IF-2017-EF research project (hellomscaproject.eu) aiming at verifying the effects and potential criticalities of adding inner insulation layers without a water vapour barrier in historic buildings. Following this project's main goal, to test the hygrothermal performance of an historic building wall retrofitted with three different internal insulation technologies, this paper presents the extensive and highly laboured results of the entire in situ monitoring campaign, analysed and assessed also with 2D hygrothermal numerical simulations. The differences between the monitored data and simulations corroborate other authors studies and suggestions [25], emphasize the need of in situ studies, reinforcing likewise other studies on the frailties of hygrothermal simulation, namely [17].

In section 2, the materials and methods used in this research are described, as well as the case study. After, in section 3, the results and the discussion of both the in situ monitoring campaign and the

simulations are presented, including variations to the tested stratigraphy via simulation, before the conclusions in section 4.

Though Italy has been in the forefront of the "energy efficiency in historic buildings research" [26] (p.72), to the authors best knowledge, this is the first study of its kind ever implemented in Italy.

2. Materials and methods

2.1. The case-study

To assess the hygrothermal performance of various thermal insulation technologies applied to historic masonry walls, an in-situ laboratory was placed into a 15th century building in Ferrara, Italy.

The building, namely the Palazzo Tassoni Estense is a listed building, which is part of an UNESCO site [27]. Located on the SE part of the city, nearby to the medieval urban walls, the "complex of the Palazzo is located in the NW part of a block, currently housing the Department of Architecture of the University of Ferrara" [28] (p.5). It is therefore representative of a public type building, with significant heritage value and widespread throughout a great area of Northern Italy.

Though the building has recently been subjected to an architecture project and a scientific restoration intervention [29], the experiment was conducted in an area of this complex that has not yet been refurbished. Therefore, the selected room, which is located on the ground floor nearby to an inner courtyard, is naturally ventilated and does not have any heating or cooling system provided.

The selected wall in which the tests were conducted is E/SE oriented, located under a porch (Fig. 1). As declared in [30] (p3), although this factor restrict the extrapolation of the study's results, it also presents a unique feature of walls alike in historic buildings: these walls do not get wet unlike most walls exposed to rainwater, neither do such walls dry as easily, since they do not receive direct sunlight. In other words, the phenomenon is studied in its purest state, as it depends solely on the vapour transport phenomena.

Thanks to a visual survey and the studying of historic documents, it was possible to identify the type of bricks used for its original construction. The "Bolognese" type (28x14x6 cm) was commonly used in buildings in the same geographical area, with analogue characteristics. The dimensions of the joints, even if quiet variable, present an average thickness of 2 cm. The overall thickness of the wall is 32 cm, including the internal and external plaster. The calculated U-value, estimated in steady state conditions, before the installation of any insulation materials was 1.44 W/m²K.

The region of Emilia Romagna (where the case study is situated) has a humid temperate climate with very hot summers (Köppen-Geiger Cfa classification [31]). The climate is characterized by a wide annual temperature range with average temperatures low in the winter (-1°/2 °C) and high in the summer (the average summer highs range from 25 °C to 28 °C). In the cold season, minimum temperatures can reach several degrees below zero at night and sometimes remain negative or close to zero even during the day (especially in the case of fog) in the winter. In the summer instead, the maximum temperatures can reach peaks of 38 °C or higher.

In addition, the Italian territory has been subdivided into 6 climatic zones according to "degree-days"(DD), that is the average climate of the municipality regardless of its geographical location [32]. The "degree-days" corresponds to the sum, extended to all the days of the year, of the difference (only positive), between the temperature of the internal environment (considered 20 °C) and the daily external temperature. According to this classification, Ferrara belongs to the "climatic zone E" with $2101 \leq DD \leq 3000$.

Fig. 1. Palazzo Tassoni Estense: the selected wall for the hygrothermal in situ analysis is located under a porch, in the courtyard of the building: a) Courtyard view, b) external view; b) internal view.

This climate context requires a verification of the hygrothermal performance of the wall, both in the winter period in the presence of low temperatures and potentially resulting in problems of frost damage and interstitial condensation, and in the summer to verify the benefit of high temperatures in the drying process of wet envelopes.

2.2. The insulation technologies

As declared in [30] (p3), the choice of the insulation materials was dictated by the drive to test commonly widespread products and solutions in the (Italian) market, suitable for both HB and new or recent buildings. The choice started from widespread materials, of which the advantages and disadvantages are well known, in order to evaluate their feasibility for use in historic buildings. So then, the selection and installation methods were discussed with the national conservation authorities along with the product's companies, through the establishment of technical worktables [33].

The choice of the final stratigraphy was made by considering: i) the kind of material and how it is linked to the historic wall (following the criteria of distinguishability, compatibility, reversibility

and "minimum intervention"); *ii)* the material's thickness (to guarantee a good insulation level, to limit the indoor space wasted and to mediate between the wet and dry periods); and the *iii)* material distribution in the market.

The final installation of the technologies was determined after the weighing up of all the advantages and all of the disadvantages of the various solutions, mainly according to the balance between: i) the energy efficiency and the width of the technology to reach a U-value which justifies the refurbishment intervention, not necessarily complying with the legislation, but leading to a performance improvement together with conservation requirements; ii) the preservation aspects, limiting the final thickness of the insulation solution and application of the materials / installation method; and iv) the hygrothermal aspects, because no vapour barrier was added to limit the summer drying potential of the historic wall or not to constrain the subsequent presence of humidity already in the wall, [34].

The ultimate decision led to the selection of calcium silicate (mineral foam) blocks, cork boards and stone wool panels, to have respectively, a material with a finishing in continuity with the historic one, a biological and traditional material, used in a innovative way and a material very wide spread in the market, characterised by a "dry installation".

The three selected solutions are briefly presented in Table 1. In Fig. 2, instead, the layout of the insulation technologies on the inner side of the historic wall is exhibited. None of these provide a vapour barrier. As shown, for each insulation strategy, the reached U-value varies. As known, in Italy as in many other European countries, the general approach when leading with historic buildings, is "performance enhancement" instead of "adaptation to standards", so professionals are not obliged to reach a certain compliance value. On the contrary, they are urged to achieve a compromised solution in equilibrium between the energy efficiency improvement and the impact on the original wall structure of a HB.

2.3. The monitoring system and sensor placement

The newly developed system to monitor the experiment has been fully described in [35]. In summary, a non-commercial setup was settled for the assessment of the hygrothermal behaviour of the internally insulated historic walls, based on Temperature (T, °C) and Relative Humidity (RH, %) combined sensors (Telaire T9602, Amphenol Thermometrics, Inc. St. Marys, PA, USA). The Data Acquisition system is based on a Master Slave configuration [28], remotely controlled. The sensors accuracy [35] is presented in Table 2.

Sensors were placed in different points of the stratigraphy of the three technologies, as exemplified in Fig. 3. Moreover, the authors tried to go beyond the work developed in [21]: instead of one single measuring point at each level of the stratigraphy, in HeLLo two monitoring levels were defined, at 1.90 m and at 3.40 m from the floor, respectively. In this way, it was possible to: i) minimize the potential influence of water capillarity at the basis of the wall [30]; ii) investigate if the behaviour of the historic wall is exactly the same at different heights; and iii) explore the performance of spaces with tall ceilings, a physical characteristic of rooms in HB. Historic walls of buildings which have been occupied throughout the years with different uses are likely to have suffered interventions and might not perform homogenously, therefore the possible changing of behaviour should be studied. Augmenting the sample of the observation points increases the possibility of implementing discussion and analysis, contributing to enrich the scientific discussion.

In the present study, the most critical point of the stratigraphy is explored, i.e. the point where the condensation is most likely to occur - in between the material's insulation layer and the historic wall (points 1 and 5 in Fig. 3). In-situ data monitoring was collected every minute. Hourly averages were generated to perform the hygrothermal simulations (all data is presented in the results section of the paper).

2.4. Climate conditions and the monitoring period

As presented earlier, the experiment was carried out inside a 700 m^3 naturally ventilated room, with no heating or cooling system in place. Therefore, aiming to improve the experiment's sustainability, to minimize the impact of the experiment on the walls and to overcome the need of the entire room's conditioning, two in situ climatized metering hot boxes were built, pretending to simulate 'standard' indoor environments.

The conditions inside the metering hot boxes were set up following the directions of several standards/guidelines (e.g. EN ISO 7730 [36], EN ISO 13,788 [37], ISO 17772–1 [38]). Temperature (T_a) and Relative Humidity (RH) were respectively $T_a \approx 20$ °C, RH $\approx 55\%$ that potentially guaranteed a satisfying ΔT_a between the indoor face of the monitored wall and the external site conditions (the outdoor climate) [28]. In particular, the EN ISO 13,788 [37] indicates that in the absence of well-defined controlled, measured or simulated indoor air conditions, to define the indoor RH set-up for heated buildings, a simplified method can be used in relation to the outdoor temperature and in relation to the crowding (internal occupancy) of the building. Therefore, in accordance with the standard, considering that an outdoor temperature varies between 0 °C and 10 °C (the winter period in the climatic condition of Ferrara) and a "standard" crowding, RH is $\approx 55\%$.

The full design and construction descriptions of these boxes (2. 50 × 2.50 × 4.01 m gross), allowed the studying of up to two insulation systems in parallel, which can be found in [28]. To create the microclimate inside each box, a 2000 W heating convector and two ultrasonic humidifiers were provided (this equipment is also fully described in [28]). The relation between the room and the hot boxes is synthetized in Fig. 4. The box's dimensions were determined also by the want to install, in parallel, two insulation systems, as depicted in Fig. 5, alike to the experimental study developed by Kloseiko et al. [20]. This study was taken as a point of reference, where different insulation systems, measuring 1.00 m width each, were studied by placing sensors in the middle (a 0.50 m distance from each material border was assured, ensuring sensors safety distance from the borders. In other words, the extension of the insulation surface is enough to minimize the impact of the influence of the material's boundaries).

The stone wool experiment was conducted in box 1, while calcium silicate blocks and cork were tested in box 2. The insulation technologies, applied on the indoor façade according to Fig. 2, occupy an approximate area inside the box(es) of: a) CaSi – 4 m^2; b) CB – 4 m^2; c) SW – 8 m^2 (Fig. 5).

In this paper a ten and a half-month period is presented, corresponding to the monitoring campaign running from November 15th 2019 until September 30th 2020. The campaign was divided in two phases: the "active monitoring phase" and the "passive monitoring phase". The period between 15th November 2019 and 12th March 2020 is referred to as the "active monitoring phase". During this phase the metering hot boxes were heated and humidified (like a proper indoor environment, i.e. there was a significant ΔT and ΔRH between the boxes and the room). Despite the common heating period which was foreseen to be until 15th April, the boxes' indoor environment conditioning was turned off on 12th March because of the COVID-19 pandemic (the University building could no longer be accessed and therefore the indoor environmental conditions inside the boxes were impossible to be controlled). Though the "active phase" of the experiment had to

Table 1
Physical properties of the materials of the tested wall.

| Insulation material	Technology description	Total thickness (mm)	Image
Calcium silicate (mineral foam) blocks (CaSi) *Wall estimated U-value 0,33 Wm²K (-77%)*	1 panel (100 mm) glued to the historic wall with a reversible adhesive mortar (8 mm thick), provided of a 10 mm finishing mortar layer	118	
Cork boards (CB) *Wall estimated U-value 0,44 Wm²K (-69%)*	1 board (50 mm) panel supported by its own timber structure (covered on the two faces with a thin layer of cork) punctually fixed to the historic wall, finished with 1 gypsum fibre board	62.5	
Stone wool panels (SW) *Wall estimated U-value 0,26 Wm²K (-82%)*	2 panels (40 + 60 mm) with their own steel frame (separated from the wall by the 40 mm panel to avoid the thermal bridge), and finished with one gypsum board	112.5	
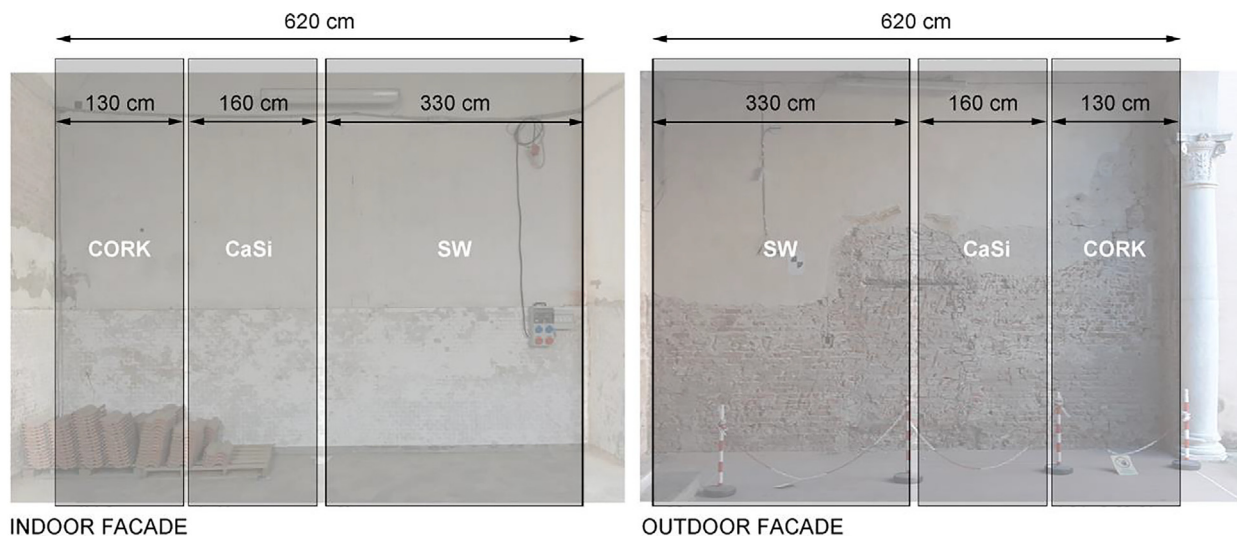
Fig. 2. Layout of the insulation distribution on the historic wall: indoor façade elevation on the left and outdoor façade elevation on the right. The extension of the tested products varies in relation to the use of two different hot boxes (see Section 2.4 for more details).

Table 2
Synthesis of sensors accuracy [35]

Temperature range (°C)	0–20	20–40	40–70
Accuracy	up to ± 1 °C	± 0.5 °C	up to ± 1 °C
Relative Humidity range (%)	0–20	20–80	80–100
Accuracy	up to ± 4 %	± 2 %	up to ± 4 %

be suspended, the remote sensing monitoring system was kept running. Therefore, from that moment started the "passive monitoring phase", with the boxes' conditioning systems switched off, running until 30th September 2020.

A synthesis of all the (hourly) monitored indoor values is presented in Table 3. As exhibited both by the average and standard deviation (sd), but also by the interquartile range (IQR), during the "active phase", the indoor environment inside both boxes was kept in quite similar conditions – mean parameter data values
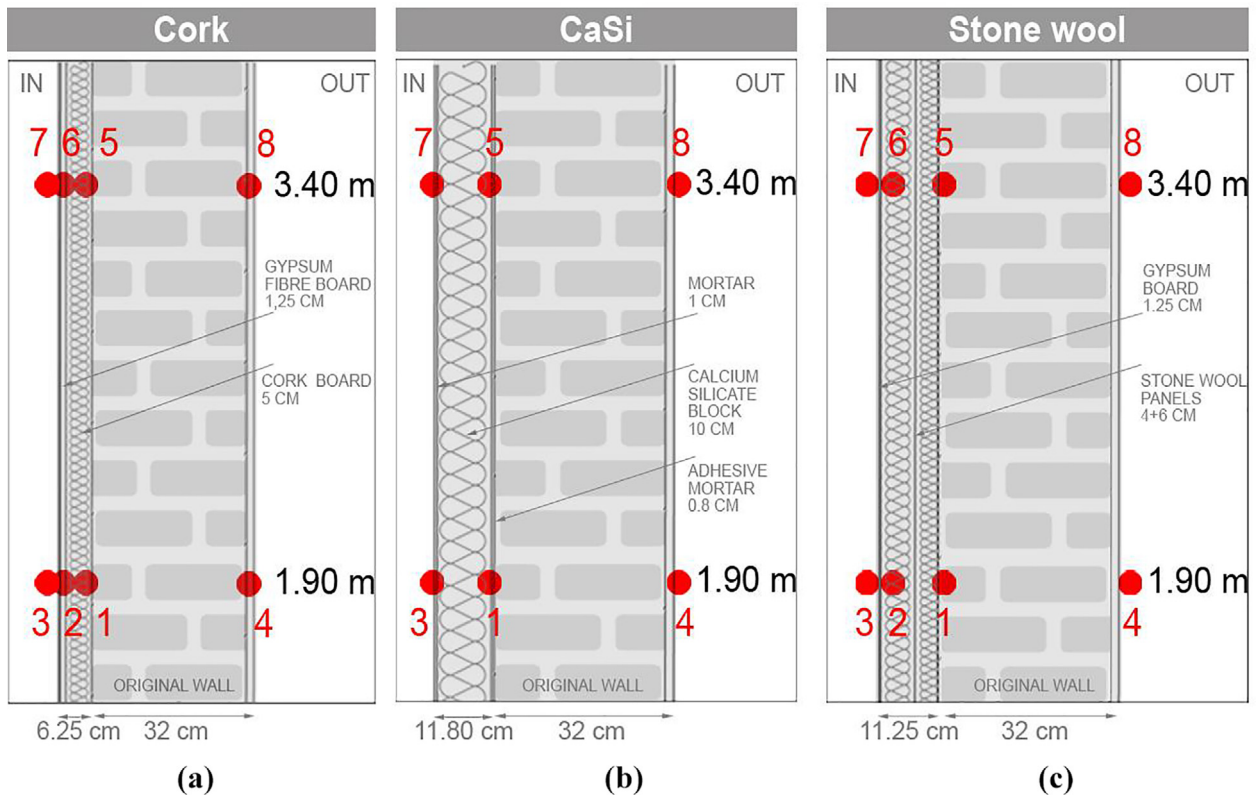
Fig. 3. Vertical section schemes of the position of the sensors: (i) sensors 8 and 4 - external surface of the original historic wall (HW); (ii) sensors 7 and 3 - internal surface of the insulation materials (placed on the internal face of the HW); (iii) The remaining sensors are placed in between the stratigraphy layers of the insulation technologies. Materials: (a) Cork boards panels (CB); (b) Calcium silicate blocks (CaSi); (c) Stone wool boards (SW).
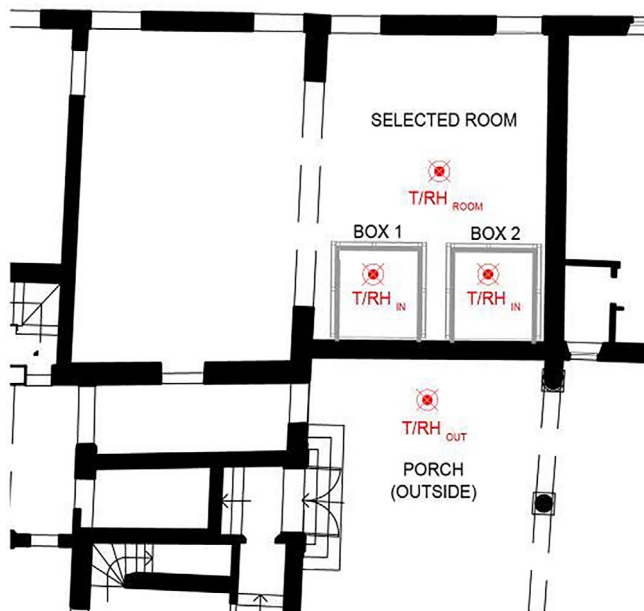

Fig. 4. Selected room (plan view) for tests and the location of the two monitoring boxes. Relative positioning of the T/RH sensors of the monitoring system (in red) of the environmental conditions (Outside – under the porch; selected room – a non-climatized indoor environment; inside – climate chambers: box 1 and box 2).

were not very spread out. Although there was slightly more variation in box 2 than in box 1, it can be stated that the environment inside the boxes was controlled.

In the framework of this research, the outdoor climate was also monitored. Due to the specific location of the studied wall - under a porch of the courtyard of the building, only T and RH values were monitored, as rain and solar radiation action were disregarded. Outdoor monitored climate data correspond to the beginning of the experiment set up, until the end of September, therefore between 15th November 2019 and 30th September 2020.

From all of the data presented in Table 3, the numbers concerning the "passive phase" stand out, namely: *i)* although RH (%) outdoor values in Ferrara were lower in summertime, their amplitude is similar to the other periods of the year; *ii)* during this same period – also due to the absence of the active systems - , the average and IQR values relating to T (°C), unveil the similitude of these parameters in the various "environments"; *iii)* RH (%) average values in the boxes was generally higher than those of the room or outdoors, but varied much less. The IQR also stated this. This fact shows that in the absence of the active systems, inside a relatively tight environment, and especially during the cooler seasons, the vapour transmission phenomena is driven indoors.

2.5. The hygrothermal simulations

Two dimensional simulations were carried out following EN 15,026 [39] recommendations, thanks to the software Delphin 6.0.20 [22] developed at the Technical University of Dresden (TUD) by the Building Climatology Department.

The hygrothermal models were designed according to the stratigraphy sections presented in Fig. 3 (a to c). The indoor climate files (T and RH values measured inside each box) result from a combination of monitored data - between 15th November 2019 and 30th September 2020 -, with EN 15,026 [39], for the period between 1st October and 14th November (signalled by the light
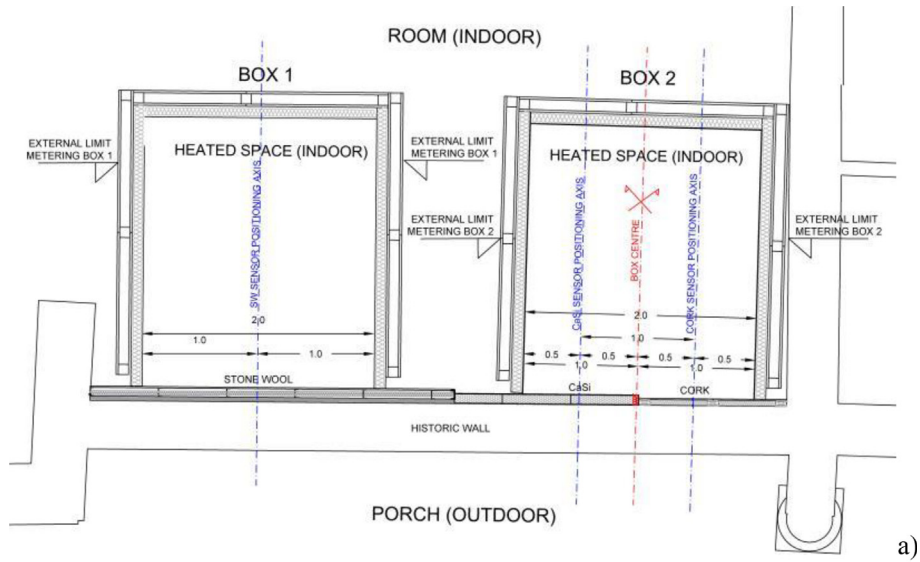
a)

b)

Fig. 5. a) Positions of the two metering hot boxes and the insulation technologies, b) The two metering boxes in the test room.

Table 3
Synthesis of the indoor environmental monitored values between 15 Nov 19/11Mar 20 (lines 1 and 2) "active phase", and 12 Mar 20/30 Sept 20 (lines 3 and 4) "passive phase"

		Box1		Box2		Room			Outdoor	
		T (°C)	RH (%)	T (°C)	RH (%)	T (°C)		RH (%)	T (°C)	RH (%)
Active phase										
1	Average ± sd	20.8 ± 0.6	55.5 ± 4.5	20.2 ± 0.5	54.0 ± 3.6	9.5 ± 2.2	68.6 ± 9.3	8.2 ± 3.2	78.5 ± 13.2
2	Interquartile range (IQR)	0.3	1.4	0.8	2.0	3.3	9.0	4.2	14.2
Passive phase										
3	Average ± sd	22.0 ± 5.2	64.3 ± 2.7	21.2 ± 5.0	64.7 ± 3.2	22.0 ± 5.2	55.0 ± 8.0	21.6 ± 5.9	58.4 ± 13.6
4	Interquartile range (IQR)	7.4	4.2	7.0	4.9	7.4	10.9	7.9	20.7

grey rectangle). The outdoor datafile instead, was derived both from monitored data (between 15th November 2019 and 30th September 2020) and a previously existing hourly climate dataset [30]. The graphical visualization of all this data is shown in Fig. 6.

For the construction of this model, all the data regarding building materials was selected from Delphin®'s Material Database 6.0.20 [22]. In particular, the parameters regarding bricks and exterior plaster refer to historic materials, as defined by the 3enCult European Project [40]. The hygrothermal characterization of the insulation stratigraphy, instead, comes from the discussion with the companies involved in the HeLLo project which lead to the following different approaches:

- *CaSi*. The material already available in the Delphin®'s Material Database corresponds exactly to the installed material. For this reason, it was simply selected from the list;
- *Cork*. The material already available in the Delphin®'s Material Database was used in the absence of the lab tested hygrothermal installed material;

- *Stone wool*. The characterization was performed in the laboratories of the Fraunhofer IBP (Institute for Building Physics) [41]; for this reason, data was appropriately formatted to fit the characterization of the "new" material of the Delphin® database.

The main properties of all the materials are shown in Table 4. The simulation models of the three insulation technologies were calibrated using field measurements. A satisfactory relation between the calculated results and the in-situ data was achieved.

3. Results and discussion

3.1. Data presentation: In situ monitoring and simulation

In the following paragraphs, the results of the monitoring phase and the simulations are presented for each material technology. Some of the reading information is common for each of the material's results:
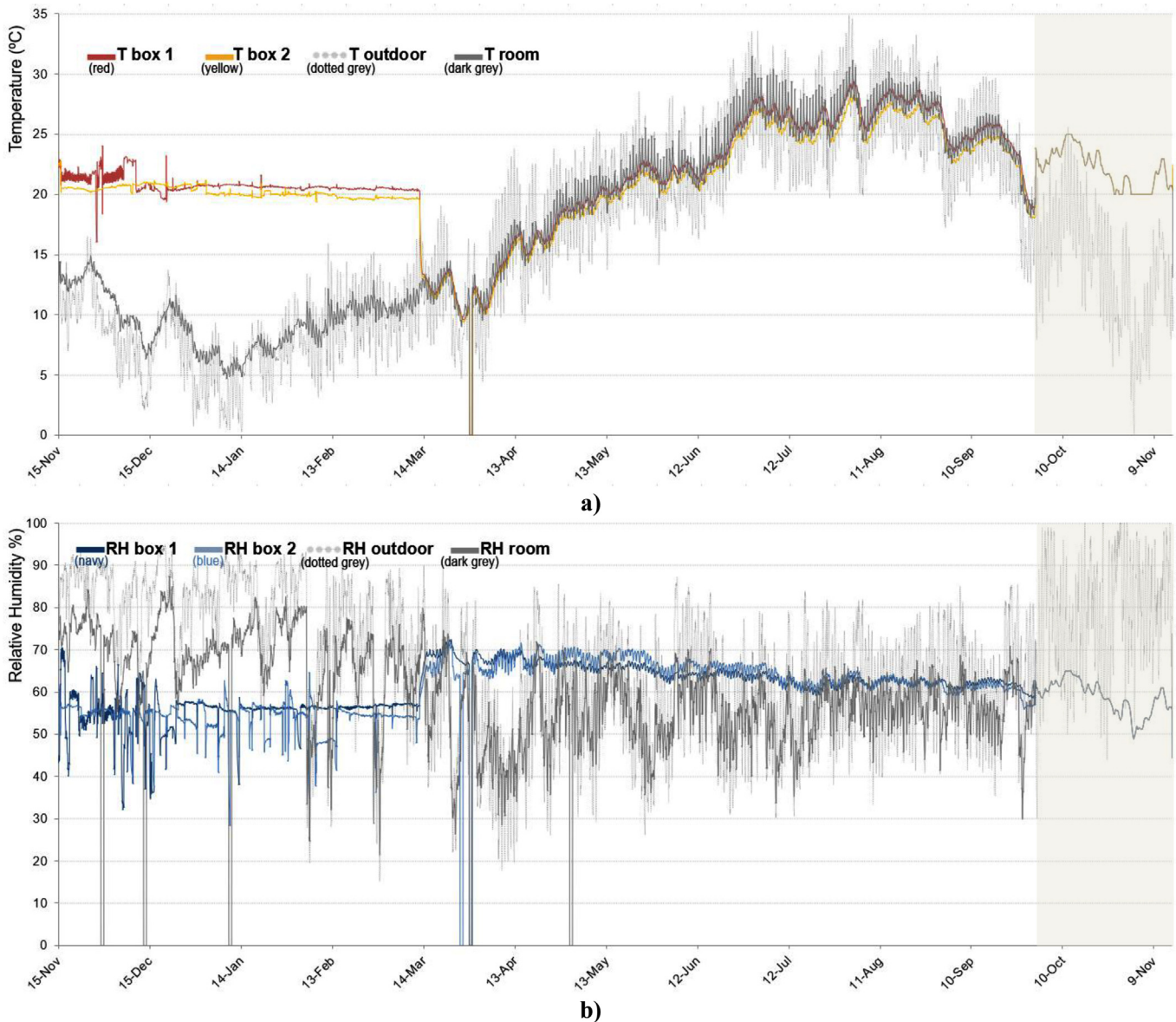

Fig. 6. Hourly annual data of external and internal climates: (a) Temperature (°C); (b) Relative Humidity (%). The light grey rectangle refers to the climate file created with EN 15,026 [39] values (period between 1st October and 14th November).

i) between all the survey's analysed points, it was decided to show only the one relating to probable interstitial condensation, being the most significant point (points 1 and 5 in Fig. 3);

ii) graphs show the entire monitoring/simulation period. A dotted grey rectangle underlines the main heating period ("active monitoring phase"): 15th November 2019 and 12th March 2020;

iii) each graph shows: T (°C) and RH (%) measured inside the box and outdoors, with grey lines; T (°C) (orange line) and RH (%) (dark blue line) measured at 3.40 m (Fig. 7), the critical point; T (°C) (yellow line) and RH (%) (blue line) measured at 1.90 m (Fig. 7), the critical point; and the simulated data (green line).

iv) As the T (°C) values outdoors, under the porch, were never negative, neither were those in either of the sensors placed at the "critical point", so, frost damage was disregarded (and it was not even assessed through simulation).

Additionally, some variations in simulations are proposed for each stratigraphy, starting from the specific need from the conservation authorities, aiming at enriching the discussions on the experimental results and to present variations to the monitored configurations.

3.2. Calcium silicate (mineral foam) blocks (CaSi)

Hourly averages of all the monitored and simulated *CaSi* values between 15th November and 30th September are presented in Fig. 8. There was no significant difference between T (°C) measured at 3.40 m or 1.90 m in between the insulation (CaSi) and the historic wall (this difference fits in the sensor accuracy which stays within 20 °C). Moreover, in these points (point 1 and 5 in Fig. 3.b), the T (min ÷ max) values, varied between 6.65 °C ÷ 29.17 °C at 3.40 m, and 6.32 °C ÷ 29.10 °C at 1.90 m.

In the case of the RH (%), at both measurement points, it was always below 95%. Nonetheless, it is worth mentioning that the sensor accuracy over 80% decreases and therefore the 95% threshold for condensation might have been achieved. For the same reasoning, RH (%) monitored differences at both levels should not be considered significant: RH (min ÷ max) values, varied between 65,08%÷93.86% at 3.40 m, and 63.19%÷90.40% at 1.90 m, respectively. Nonetheless, the initial building moisture and successive drying out period was visible: RH (%) between the insulation and the historic wall decreased until 1st October 2020, reaching values below 65%.

Additionally, the in situ data was compared with the simulation. It was verified that the simulated values over dimensioned the monitored T (°C), especially in the spring-summer season: the global difference between the measured (average of the two sensors) and the simulated values varied between 0.00 °C ÷ 5.16 °C and RMSE = 2.71 °C. During the "active-phase", the RMSE = 0.67, which is comparable with the instrumental error (±1 °C when 0 ≤ T (°C) ≤ 20). In this case, the RMSE is even lower than the sensors accuracy.

On the contrary, the RH (%) simulated values were underestimated. The field data showed higher RH (%) values than those suggested in the simulation. It is likely that the underestimation of RH (%) by the software is caused by the overestimation of inter-seasonal drying. Both the field and the simulation data showed

Table 4

Main hygrothermal properties of the chosen materials. Density (ρ), specific heat (Cp), porosity (θ**por**), thermal conductivity (λ**dry**), vapour resistance (μ**dry**) and capillary absorption coefficient (Aw).

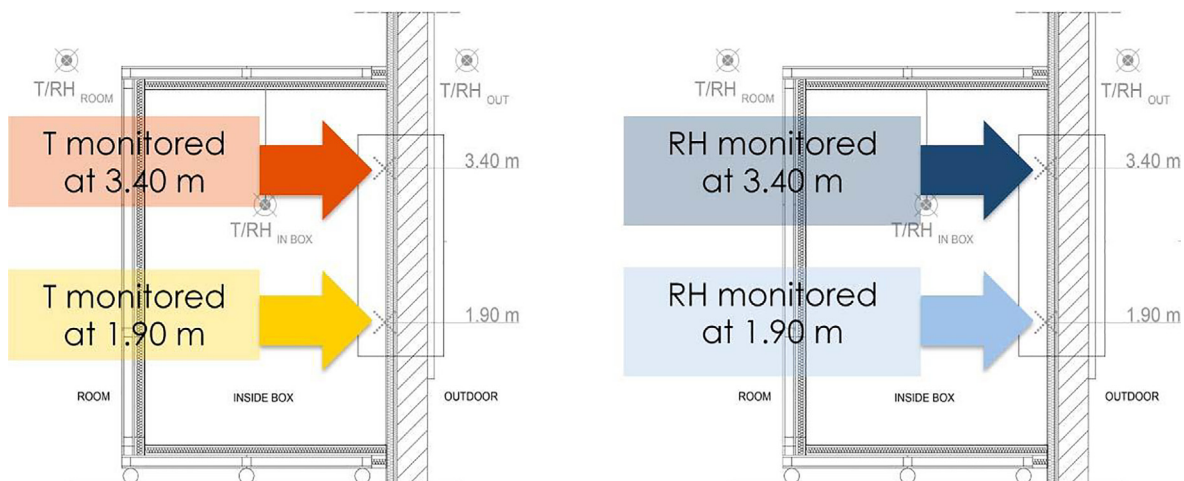| Material	ID Delphin DB	ρ[kg/m³]	C$_p$[J/KgK]	θ_{por}[m³/m³]	λ_{dry}[W/mK]	μ_{dry}[-]	A$_w$[kg/m²s05]
Lime Mortar	143	1570	1000	0.408	0.7	11.0	0.176
Historical Brick (*)	532	1759	1092	0.336	0.624	24.5	0.184
Lime plaster External (*)	520	1604	869	0.395	0.69	19	0.179
Lime plaster Internal	629	1498	802	0.435	0.412	9.3	0.018
Calcium silicate (mineral foam)	596	126	968	0.951	0.045	5.7	0.004
Glue Mortar (for Mineral insulation Board)	77	830	815	0.685	0.155	13.0	0.003
Gypsum fibre board	413	1133	1228	0.626	0.341	16.8	0.057
Thermocork	418	114	2253	0.957	0.047	28.9	0.009
Oak	458	588	1584	0.630	0.212	9.6	0.016
Stone wool	–	70	1030	0.950	0.033	1	–
Steel	238	7800	470	–	47	–	–
Gypsum board	599	745	1826	0.719	0.177	11	0.179

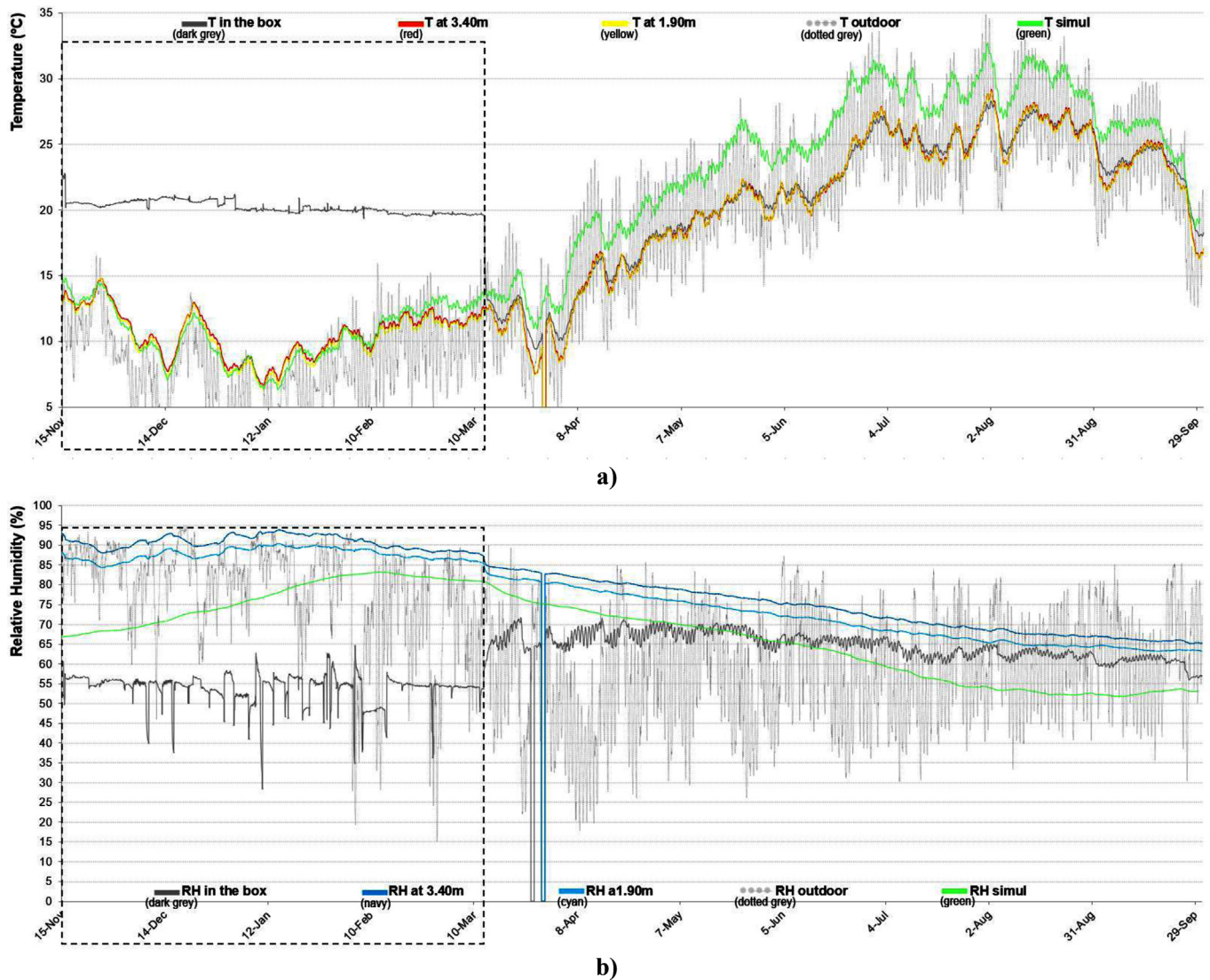**Fig. 7.** Reading scheme of the monitoring/simulation's graphs.

Fig. 8. Hourly monitored and simulated hygrothermal conditions, between 15th November and 30th September with *CaSi* insulation technology (118 mm), at the probable condensation point: a) T (°C); b) RH (%).

an apparent seasonal dependency – higher RH (%) values in the winter and lower in the summer. Statistically, the global difference between the measured (average of the two sensors) and the simulated values varied between 3.36 % ÷ 23.71 % and RMSE = 11.66 %. When analysed separately, in both phases, active and passive, the RMSE value was more than the double of the instrumental error. Nonetheless, it is worth to mention that such error increases up to ± 4 % when RH ≥ 80%.

3.3. Cork boards (Co)

Co hourly data, monitored and simulated, between 15th November and 1st October, are presented in Fig. 9. No significant difference between the T (°C) measured at 3.40 m or at 1.90 m in between the insulation (Co) and the historic wall (as the difference fits the sensor accuracy which stays within 20 °C) was verified. Moreover, in these points (point 1 and 5 in Fig. 3b), the T (min ÷ max) values, varied between 7.89 °C ÷ 29.03 °C at 3.40 m, and 8.01 °C ÷ 29.47 °C at 1.90 m.

RH (%) values were always below 80%, therefore, the risk of condensation was clearly never present. Herein, RH (%) differences

measured at both heights was observed, RH (min ÷ max) values, varied between 60,67%÷76.30% at 3.40 m, and 53.77%÷60.20% at 1.90 m, respectively. In other words, the maximum RH (%) value registered at the lower sensor equalled the minimum value registered at 3.40 m.

The simulation overestimated the T (°C) values: the global difference between the measured (average of the two sensors) and the simulated values varied between 0.00 ÷ 3.73 and, RMSE = 2.01. During the "active-phase", RMSE = 0.87, which is lower than the instrumental error. In some moments the simulation overestimated the onsite RH (%) behaviour, in others it underestimated it. This difference was re-emphasized by the end of July. Statistically: the difference between the RH (%) measured (average of the two sensors) and the simulated values varied between 0.00 % ÷10.38 % and RMSE = 5.92 % – this value is higher than the sensors accuracy. As visible in Fig. 9.b), the RH (%) simulation curve better fitted the data registered by the sensor placed at 3.40 m during most of the time. If data had been collected solely at 3.40 m, and the same analysis was performed, the difference would be lower 0.00 % ÷ 8.10 %, and RMSE = 3.96 %, fitting the instrumental error ± 2 % when 20 ≤ RH (%) ≤ 80.
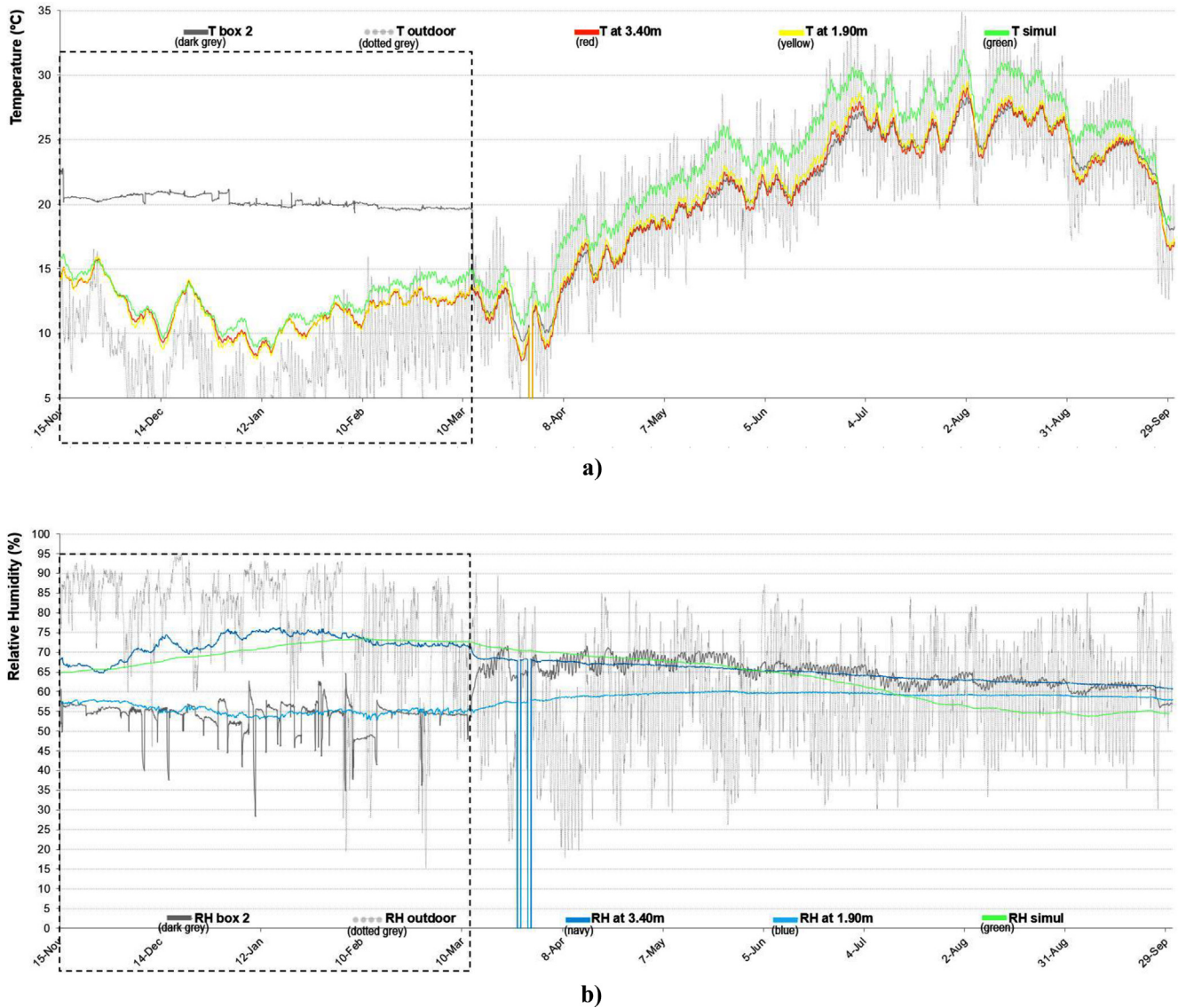
Fig. 9. Hourly monitored and simulated hygrothermal conditions, between 15th November and 30th September with *Co* insulation technology (62.5 mm), at the probable condensation point: a) T (°C); b) RH (%).

3.4. Stone wool panels

Part of the results of this insulation technology were previously divulged in [30]. Previously, only a short 3-month monitoring period was presented and discussed. Herein, Fig. 10, shows the entire dataset.

The T (°C) profile of the monitored data was not very different from the other materials, i.e., no significant difference was found between T (°C) measured at 3.40 m or at 1.90 m, at the likely condensation point. At these points, the T (min ÷ max) values, varied between 6.53 °C ÷ 30.18 °C at 3.40 m and 5.78 °C ÷ 29.76 °C at 1.90 m.

RH (%) was not so "homogeneous". A visible difference was found between the RH (min ÷ max) measured at 1.90 m, 64.12%÷85.24% and 3.40 m, 62.15%÷94.19%, respectively. Although the condensation limit (95%) was never reached, much like with the *CaSi*, a reasonable doubt can be noted, due to sensors accuracy over 80%.

Concerning the simulation, much like in the previous technologies, when it comes to the T (°C), the simulation overestimated the T (°C) values, especially after the springtime: the global difference between the measured (average of the two sensors) and the simulated varied between 0.00 °C ÷ 4.49 °C and RMSE = 2.06 °C. During the "active-phase", the RMSE = 0.56, which is comparable with the instrumental error (±1 °C when $0 \leq$ T (°C) ≤ 20). In this case, the RMSE is even lower than the sensors accuracy.

During a considerable part of the year, the RH (%) simulation curve either overestimated or underestimated the field data. Statistically, the global difference between the measured (average of the two sensors) and the simulated values varied between 0.00 % ÷ 12.87 % and RMSE = 7.50 %. If only the "active-phase" was observed, RMSE = 5.93 %, approaching the instrumental error (up to ± 4 % when RH $\geq$ 80%). From the observation of Fig. 10.**b)**, it is visible that the simulation curve (RH, %) better fitted the monitored values at 3.40 m. If data had been measured solely at 3.40 m, the difference between the simulation and the monitored data would
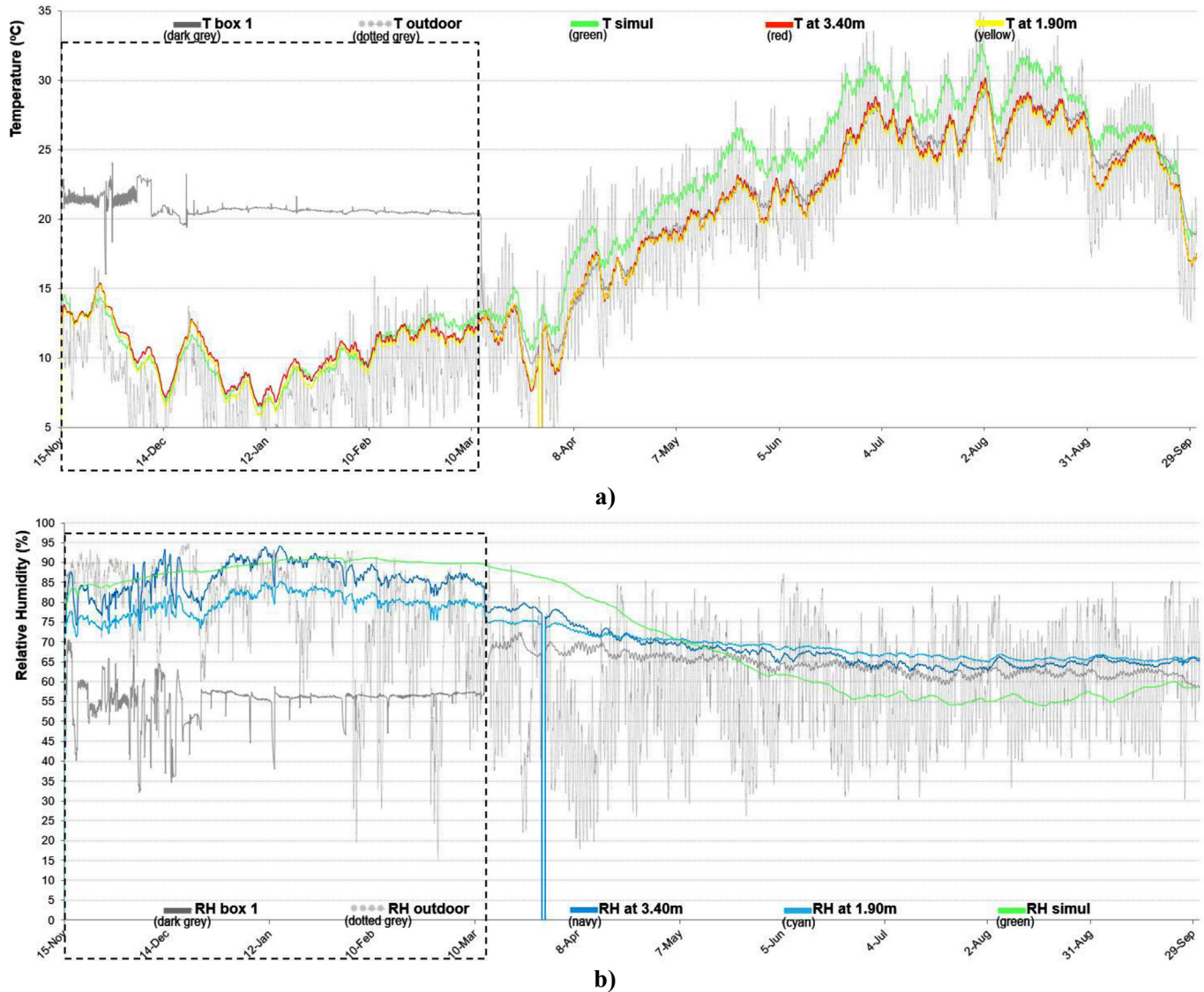
Fig. 10. Hourly monitored and simulated hygrothermal conditions, between 15th November and 30th September with SW insulation technology (112.5 mm), at the probable condensation point: a) T (°C); b) RH (%).

be less significant: 0.00 % ÷ 11.68 % and RMSE = 6.32 %. If only the "active-phase" was observed, RMSE = 4.12 %, fitting the instrumental error ± 2 % when 20 ≤ RH (%) ≤ 80.

In sum, differences were found between simulated and monitored data in all models. The lowest RMSE values were found in *Co* simulations. Some general observations can be drawn:

- Generally, the simulated data better fitted the in-situ data in the "active-phase" rather than on the "passive" one. This tendency was stronger for T (°C) rather than RH (%). This can be due to the daily fluctuations of the outdoor temperatures (day / night) which are less pronounced than in periods of high and uncontrolled temperatures (passive phase);
- In the cases of *Co* and stone wool panels, the simulation better fitted the data that was collected at 3.40 m;
- The differences between the in-situ and the simulation data can be due to the non-homogeneity of the historic wall and /or the underestimated thermal inertia of this wall (likely higher) and/ or the simulation might not be perfectly parameterized. For example, the materials characteristics, such as porosity, might not be perfectly parameterized and this might determine greater variations in RH.

As previously mentioned, with the aim of enriching this study discussion, proposing some alternatives, and improving the calibration of the hygrothermal simulation models developed for these insulation technologies, some small variations were performed in every model, as shown in the next paragraphs. In order to improve the readings of the new figures, the indoor and outdoor climate data was removed.

3.5. Variations of the simulations

3.5.1. Calcium silicate (mineral foam) blocks

As the *CaSi* insulation technology corresponds to a "wet" installation method, a few variations were introduced and new simulations were performed:

i) instead of looking at the last year of the simulation, as is common practice, authors looked at the first year of the simulated data, and compared it with the field monitoring campaign, which started after the installation;

ii) a new simulation was run, changing the initial RH (%) value, from 80% to 95%;

iii) another simulation was run with a different adhesive glue mortar;

iv) one last variation was performed reducing the material width to 6 cm.

Concerning [*i*], the temperature of the simulated data of the first year, when compared to the last year of the simulation (Fig. 8.**a**), did not differ significantly and therefore it is not shown (max ΔT = 0.1 °C). RH (%) values, instead, were quite different (max ΔRH = 15 %) and, therefore, this data is presented in Fig. 11. As exhibited by the pink broken line, the RH simulation of the first year is closer to the in-situ data, considering that this corresponds to the initial months after the installation. Nonetheless, the simulation data underestimates the field measurements almost throughout the entire monitoring period.

Given the obtained results from the initial simulation and its first variation, the second action [*ii*] was changing the initial RH (%) value of the simulation, from 80% to 95%. Once again, in terms of T (°C), no significant difference was noticed (max ΔT = 0.4 °C). In terms of RH (%) some variations are found (max ΔRH = 27 %): the data of the first year overestimated the RH (%) behaviour profile, while the last year's data overlapped with the initial simulation, underestimating the values of the data collected in situ. In other words, whether the initial RH value is 80% or 95%, if solely the data of the last year is observed, from any of the simulations, the same results are obtained. That is, between variation [*i*] and [*ii*] - which aimed at bringing closer the simulation values to the monitored ones, the one that better serves the purpose is [*i*]. Consequently, no Figure is shown for [*ii*].

Notwithstanding such results, it was decided to introduce another variation, admitting 95% as the initial RH value [*iii*]: instead of using the same material in both the mortar layers, the adhesive and the finishing mortar, the adhesive layer was replaced by a clay mortar, of which the properties are shown in Table 6 (this clay mortar presents a much higher capillary absorption coefficient).

No significant differences between the original simulation and the new one [*iii*] with the clay adhesive mortar were obtained, therefore, no new figure is shown concerning this simulation. In summary, it can be stated that the different properties of the mortars induced practically no change in the final result of the generated RH (%) at the probable condensation point.

Finally, one latest variation was introduced [*iv*]: reducing the CaSi blocks width to 6 cm (to pursue the conservation requirements). Two simulations were in fact performed, considering the initial RH at 80% and at 95%.

At 80% initial value, both the data of the first year and the data of the last year of the new simulation (with 6 cm width of *CaSi*) showed slightly better results than that of the initial simulation, of 10 cm material width in the "passive phase", but worse behaviour during winter time if the last year data is observed, Fig. 12. At 95% initial RH value, if the first-year simulated data is observed, 6 cm behaves better than the construction solution currently installed (no Figure is shown to avoid data redundancy). Nonetheless, in a broader perspective, if the last year of the simulation is observed, 10 cm seems to behave better at wintertime (the most critical period of the year).

3.5.2. Cork boards
Concerning *Co*, the authors promoted three variations:

i) Simulation with a 10 cm width of thermal insulation material, cork;
ii) Simulation with two gypsum boards instead of one fibreboard;
iii) Simulation with a variation to the software's library material – the authors edited the cork material in the Delphin software's library with the thermal characteristics of the material tested in situ, as described in Table 7, "Mixed cork".

The results of the first variation [*i*] are presented in Fig. 13. As expected, augmenting the material's width, would lower the T (°C)
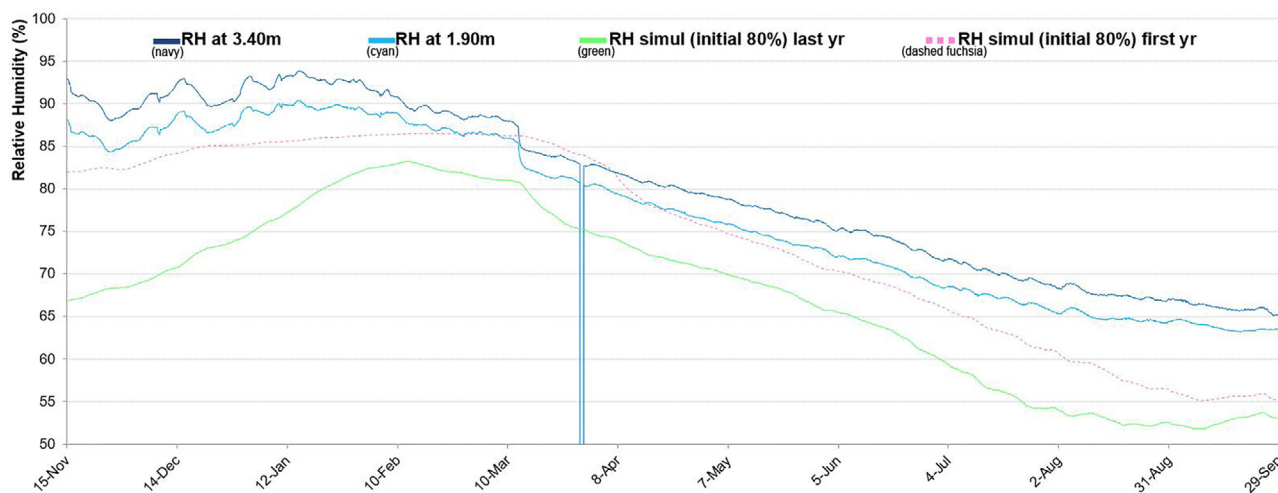

Fig. 11. Monitored and simulated RH (%) conditions, between 15th November and 30th September with *CaSi* insulation technology, at the probable condensation point [original simulation and scenario *i*)].

Table 6
Main hygrothermal properties of the two kind of mortars used for CaSi blocks simulation density (ρ), specific heat (Cp), porosity (θ_{por}), thermal conductivity (λ_{dry}), vapour resistance (μ_{dry}) and capillary absorption coefficient (Aw).

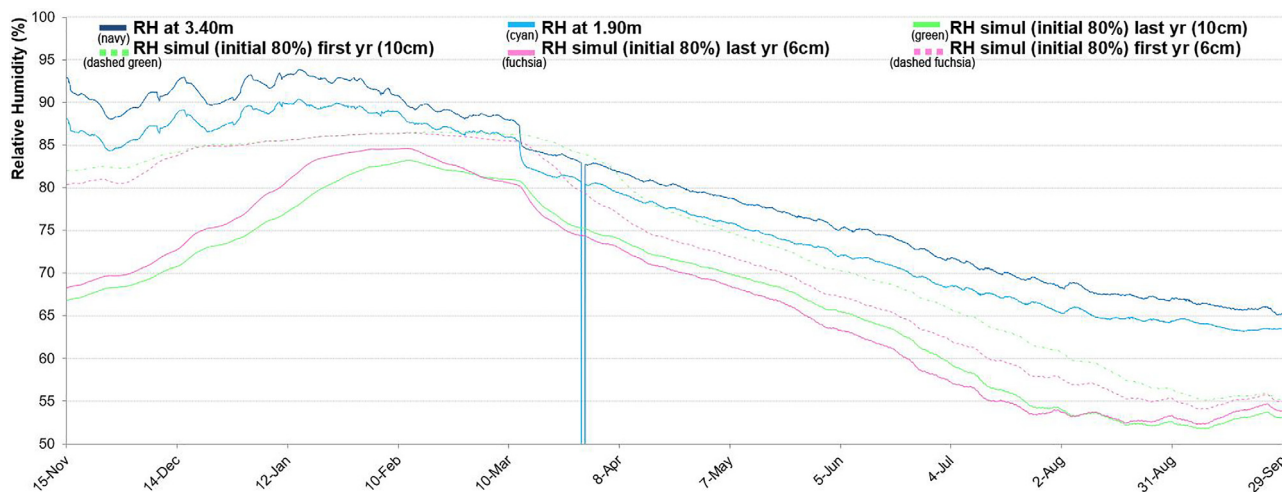| Material	ID Delphin DB	ρ[kg/m³]	C_p[J/KgK]	θ_{por}[m³/m³]	λ_{dry}[W/mK]	μ_{dry}[-]	A_w[kg/m²s05]
Glue Mortar (for Mineral insulation Board)	77	830	815	0.685	0.155	13.0	0.003
Clay Mortar (historical)	128	1568	488	0.468	0.582	11.4	0.176

Fig. 12. Monitored and simulated RH (%) conditions, between 15th November and 30th September with *CaSi* insulation technology, at the probable condensation point [original simulation and scenario *iv)*, with initial RH value equal to 80%].

Table 7
Hygrothermal properties of cork used in the simulation. Density (ρ), specific heat (Cp), porosity ($\theta_{\mathbf{por}}$), thermal conductivity ($\lambda_{\mathbf{dry}}$), vapour resistance ($\mu_{\mathbf{dry}}$) and capillary absorption coefficient (Aw).

Material	ID Delphin DB	ρ[kg/m³]	C_p[J/KgK]	θ_{por}[m³/m³]	λ_{dry}[W/mK]	μ_{dry}[-]	A_w[kg/m²s05]
Thermocork	418	114	2253	0.957	0.047	28.9	0.009
"Mixed cork"	–	**160***	**2100***	**0.9***	**0.042***	**10.7***	0.009

(*) The values in bold correspond to the thermal properties values of the cork provided by the company.

at the probable condensation point, as the heat transferred from the "indoor environment" would have to cross a higher insulation width (max ΔT = 1.8 °C). In terms of RH (%), the achieved maximum value would be lower than when the 5 cm width was tested in wintertime, reaching practically the same values during the drying-out phase, as observable in Fig. 13.**b**) (max ΔRH = 3.2 %).

The outputs of the new simulation [*ii)*], two gypsum boards finishing, introduced practically no change: the hygrothermal curves obtained with the two gypsum boards practically overlap those generated with one single fibreboard. Only during wintertime, it could be observed that there is a very slight increase of the RH (%) value (max ΔT = 0.4 °C; max ΔRH = 2.6 %). Due to the insignificant differences, no figures are presented.

Finally, concerning [*iii)*], no significant differences were observed in terms of T (°C), therefore no data is shown, but smoother RH (%) values were obtained, as evidenced in Fig. 14, when compared with the original simulation.

3.5.3. Stone wool panels

In [30], the authors have already proposed a few simulation variations, namely: *i)* reducing the stone wool thickness to 6 cm; *ii)* reducing the stone wool thickness to 8 cm; and *iii)* adding a second gypsum board to the internal finishing (one single layer was installed and was initially simulated). Scenarios *i)* and *ii)* showed the decrease of energy performance from that solution and a very small difference in RH (1%) at the likely condensation point. The third scenario, *iii)*, resulted in an improvement of the vapour resistance of the internal finishing, that could contribute to the reduction of the moisture accumulation during the wetting period. Nonetheless, this scenario was responsible for a delay during the drying phase.

As during the drying phase, moisture content significantly dried out from the interstitial area in all the studied simulations, herein, the authors propose a new hypothesis: an equilibrium between the energy performance reduction (reducing the insulation material by 2 cm) and an increase of the vapour resistance, balancing also the space reduction of the proposed solution: in summary, the new scenario is made of 8 cm stone wool and two gypsum boards of internal finishing. While the T (°C) results between both simulations are negligible (max ΔT = 0.3 °C, therefore not shown), RH (%) is not (max ΔRH = 5.9 %): please consider Fig. 15. During the winter period, a very smooth difference can be found between the original simulation and the new one (in terms of T, °C), but both curves overlap from springtime. In terms of RH (%), the new simulation suggests that RH (%) will always be lower than 90%, therefore reducing the condensation risk.

4. Conclusions

The paper presents the results of the evaluation, both by in situ measurements and dynamic software simulations, of the hygrothermal behaviour of three internal insulation systems for a historic brick wall. The study aimed to assess the possible condensation problems at the most critical point of the stratigraphy, between the wall and the insulation material, without the installation of any water vapour barriers, to limit the modification of the original hygrothermal behaviour of the wall.

The monitoring campaign ran between 15th November 2019 and 30th September 2020. In situ data was used for calibrating the 2D simulation model carried out with Delphin 6.0.20 software. The results mainly confirm the initial theory: under such climatic conditions, during the monitoring period and with the studied stratigraphy, both in situ monitoring and the simulation predictions evidenced no risk of frost damage to the brick wall, one possible and common problem with indoor insulation technologies. With regards to the risk of interstitial condensation, the simula-
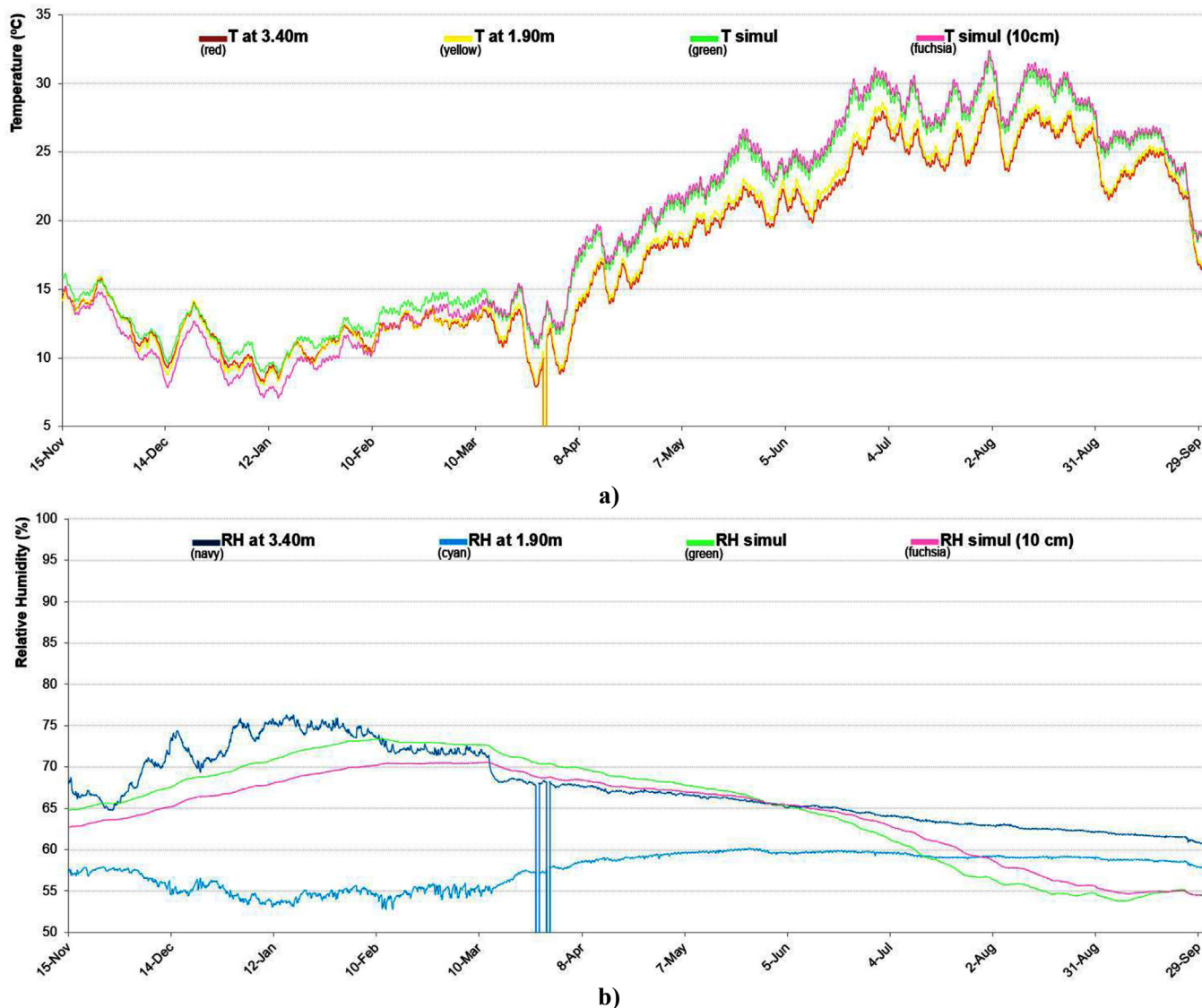
Fig. 13. Monitored and simulated hygrothermal conditions, between 15th November and 30th September with *Co* insulation technology, at the probable condensation point [original simulation and scenario *i)*].
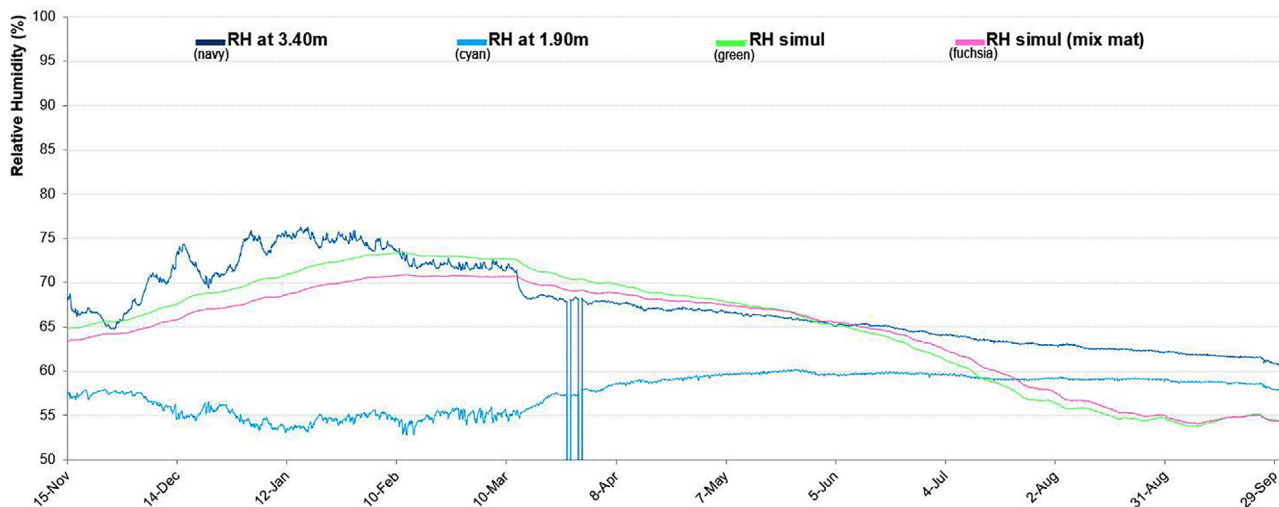

Fig. 14. Monitored and simulated hygrothermal conditions, between 15th November and 30th September with *Co* insulation technology, at the probable condensation point [original simulation and scenario *iii)*].
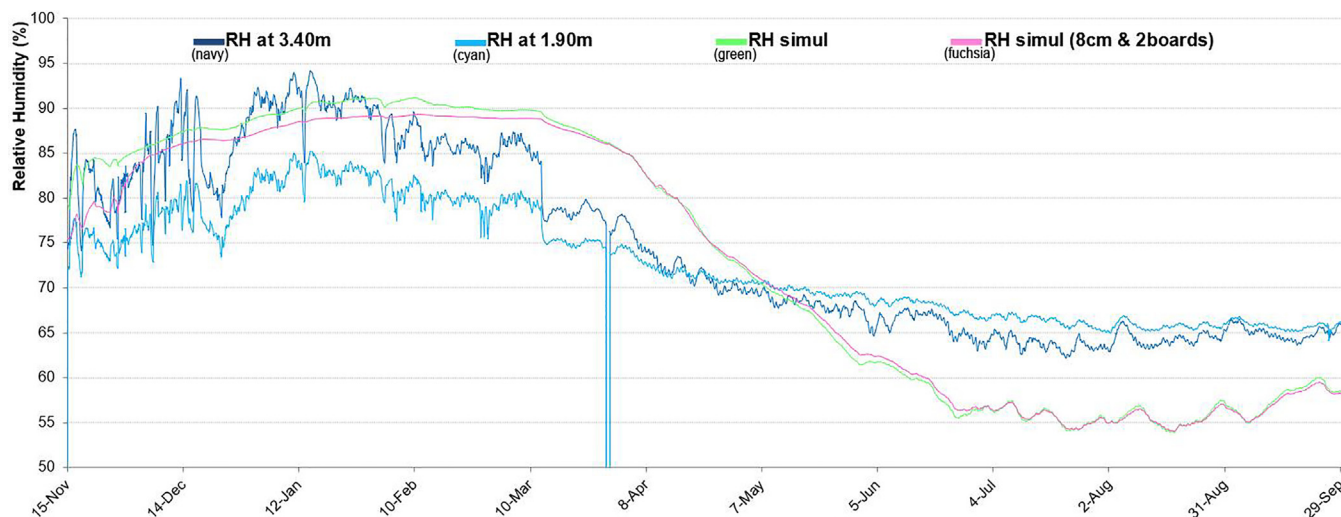
Fig. 15. Hourly monitored and simulated RH (%) values, between 15th November and 30th September with the SW insulation technology, at the probable condensation point [points 1 and 5, Fig. 3b)].

tions showed no risk even in the absence of a water vapour barrier. Some of the installed technologies presented high RH (%) values, but these were lower than the reference values in all the situations/periods. In addition, the amount of water vapour accumulated during the winter season dried out during spring/summer period. The differences between the in-situ data and the simulation evidenced that, undoubtedly, the simulation alone would not be enough to properly evaluate the interventions.

Some variations to the simulations were performed to analyse different configurations, underlining some issues: *i)* the use of 'wet installation systems' requires a longer drying period, during which the presence of moisture may influence the original hygrothermal performance of the wall; *ii)* the insulation material's thickness is a very delicate topic and should be deeply studied to understand the best balance between the energy's enhancement and moisture accumulation. In all the analysed cases, a greater thickness of the insulation corresponds to a better performance during the winter period but a more difficult drying period during the summer season. The final choice depends on the maximum RH (%) value reached during winter.

When in critical situations, as when RH (%) values are close to the admitted ones (around 95%), instead of adding a water vapour barrier, an improvement of the vapour resistance of the internal finishing (for example adding a second gypsum board), could be sufficient enough to reduce the moisture accumulation during the wetting period, in compliance with the requirements of the conservation authorities that ask to maintain, as much as possible, the original water vapour diffusion transport characteristics, of historic brick walls. In addition, the gypsum board acts as a hygrothermal flywheel, absorbing excess humidity from the indoor environment and returning it when it has dropped.

From this newly developed study, the authors can state that the absence of the vapour barrier is a possible path to be considered, in historic buildings' energy refurbishment. This means that, even in the historic context, different insulation technologies are a possibility, after an accurate analysis and balance between energy efficiency, technology thickness, conservation and hygrothermal aspects.

The development of the research steps has also confirmed several criticalities anticipated through energy modelling of historic buildings [25]:

i) in situ monitored data showed RH differences measured at different heights of the wall due to the wall texture irregularity;

ii) the simulation overestimated the T (°C) values, especially in the spring-summer seasons, demonstrating that the historic wall's thermal inertia is higher than predicted;

iii) since the T (°C) was overestimated for all the tested stratigraphy, the RH (%) simulated values were different from the monitored ones, including variations in all the situations. In particular, when the RH (%) monitored value is higher than 80%, a reasonable doubt can be appointed due to the sensors' accuracy levels, which may justify such a discrepancy.

Nevertheless, part of the criticalities is assignable to the difficulties in the characterisation of the historic materials, through the software database. In other words, the results reinforce the limitations of the materials' library software, suggesting advanced parametric studies of various coefficients which characterize these materials.

All these aspects underline the importance of the in situ analysis to increase the awareness about the hygrothermal behaviour of historic envelopes. The authors aim to continue the monitoring campaign to enrich the data collection during a longer period and in the future, to test new insulation technologies and new kinds of historic wall materials from different case studies.

Declaration of Competing Interest

The authors declare that they have no known competing financial interests or personal relationships that could have appeared to influence the work reported in this paper.

Acknowledgements

Funding

References

[1] D. Ürge-Vorsatz, N. Eyre, P. Graham, D. Harvey, E. Hertwich, Y. Jiang, C. Kornevall, M. Majumdar, J.E. McMahon, S. Mirasgedis, S. Murakami, A. Novikova, K. Janda, O. Masera, M. McNeil, K. Petrichenko, S.T. Herrero, E. Jochem, Energy End-Use: Buildings, in: E. Jochem (Ed.), Glob. Energy Assess. - Towar. a Sustain. Futur., Cambridge University Press, Cambridge, 2012: pp. 649–760. https://doi.org/10.1017/cbo9780511793677.016.

[2] DIRECTIVE 2012/27/EU OF THE EUROPEAN PARLIAMENT AND OF THE COUNCIL of 25 October 2012, Off. J. Eur. Union. L 315/1 (2012).

[3] EC, DIRECTIVE (EU) 2018/844 OF THE EUROPEAN PARLIAMENT AND OF THE COUNCIL of 30 May 2018, Off. J. Eur. Union. (n.d.).

[4] European Commission, Questions and Answers on the Renovation Wave, Oct. 14. (2020) 1–4. https://bit.ly/3ynz42w (accessed December 15, 2020).

[5] European Commission, Factsheet. What is the European Green Deal?, (2019). https://bit.ly/2T4iwN7 (accessed January 10, 2021).

[6] UNESCO, UNESCO Database of National Cultural Heritage Laws, (2003). https://en.unesco.org/news/unesco-database-national-cultural-heritage-laws-updated (accessed November 8, 2018).

[7] UNESCO, Operational Guidelines for the Implementation of the World Heritage Convention, World Heritage Centre (2021) 1–188. https://whc.unesco.org/en/guidelines/ (accessed November 14, 2021).

[8] Green Building Council Italia, Sistema di verifica GBC HISTORIC BUILDING ® Versione breve ad uso pubblico e divulgativo. Per il restauro e la riqualificazione degli edifici storici. Edizione 2016 - revisione aprile 2017, (2016) 124. https://bit.ly/2YgixxQ.

[9] Decreto Legislativo 22 gennaio 2004, n. 42. Codice dei beni culturali e del paesaggio, ai sensi dell'articolo 10 della legge 6 luglio 2002, n. 137, Gazz. Uff. Della Repubb. Ital. 45 (n.d.) Supplemento Ordinario n. 28.

[10] SFS - Swedish Planning and Building Act, 2010:900. Plan-och bygglag (In Swedish), (2010).

[11] S. Lidelöw, T. Örn, A. Luciani, A. Rizzo, Energy-efficiency measures for heritage buildings: A literature review, Sustain. Cities Soc. 45 (2019) 231–242, https://doi.org/10.1016/j.scs.2018.09.029.

[12] MiBACT, Linee di indirizzo per il miglioramento dell'efficienza energetica nel patrimonio culturale. Architettura, centri e nuclei storici ed urbani, (2015) 200. https://bit.ly/39l3qXE (accessed December 19, 2018).

[13] BS EN 16883:2017, BS EN 16883:2017 Conservation of cultural heritage — Guidelines for improving the energy performance of historic buildings, (2017). https://shop.bsigroup.com/ProductDetail/?pid=000000000030322690.

[14] ICOMOS, Future of Our Pasts: Engaging Cultural Heritage in Climate Action, 2019. https://bit.ly/330nmjI (accessed July 1, 2020)

[15] J. Toman, A. Vimmrová, R. Černý, Long-term on-site assessment of hygrothermal performance of interior thermal insulation system without water vapour barrier, Energy Build. 41 (1) (2009) 51–55, https://doi.org/10.1016/j.enbuild.2008.07.007.

[16] J. Zagorskas, E.K. Zavadskas, Z. Turskis, M. Burinskienė, A. Blumberga, D. Blumberga, Thermal insulation alternatives of historic brick buildings in Baltic Sea Region, Energy Build. 78 (2014) 35–42, https://doi.org/10.1016/j.enbuild.2014.04.010.

[17] M. Calzolari, P. Davoli, L. Dias Pereira, From the dynamic simulations assessment of the hygrothermal behavior of internal insulation systems for historic buildings towards the HeLLo project, Int. J. Environ. Sci. Dev. 11 (2020) 278–285. https://doi.org/10.18178/ijesd.2020.11.6.1263.

[18] T.K. Hansen, S.P. Bjarløv, R.H. Peuhkuri, M. Harrestrup, Long term in situ measurements of hygrothermal conditions at critical points in four cases of internally insulated historic solid masonry walls, Energy Build. 172 (2018) 235–248, https://doi.org/10.1016/j.enbuild.2018.05.001.

[19] A.A. Hamid, P. Wallent, Hygrothermal assessment of internally added thermal insulation on external brick walls in Swedish multifamily buildings, Build. Environ. 123 (2017) 351–362, https://doi.org/10.1016/j.buildenv.2017.05.019.

[20] P. Kloseiko, E. Arumagi, T. Kalamees, Hygrothermal performance of internally insulated brick wall in cold climate : A case study in a historical school

building, J. Build. Phys. 38 (2015) 444–464, https://doi.org/10.1177/1744259114532609.

[21] R. Walker, S. Pavía, Thermal and moisture monitoring of an internally insulated historic brick wall, Build. Environ. 133 (2018) 178–186, https://doi.org/10.1016/j.buildenv.2018.02.020.

[22] TU Dresden, Institut fur Bauklimatik. Delphin 6.0.20. Material database, (n.d.).

[23] M. Dondi, P. Principi, M. Raimondo, G. Zanarini, Water vapour permeability of clay bricks, Constr. Build. Mater. 17 (4) (2003) 253–258, https://doi.org/10.1016/S0950-0618(02)00117-4.

[24] European Commission, EU H2020 MSCA-IF-ES HeLLo project, (2019). https://cordis.europa.eu/project/rcn/215475/factsheet/en (accessed April 7, 2019).

[25] G.G. Akkurt, N. Aste, J. Borderon, A. Buda, M. Calzolari, D. Chung, V. Costanzo, C. Del Pero, G. Evola, H.E. Huerto-Cardenas, F. Leonforte, A. Lo Faro, E. Lucchi, L. Marletta, F. Nocera, V. Pracchi, C. Turhan, Dynamic thermal and hygrometric simulation of historical buildings: Critical factors and possible solutions, Renew. Sustain. Energy Rev. 118 (2020) 109509, https://doi.org/10.1016/j.rser.2019.109509.

[26] A. Martínez-Molina, I. Tort-Ausina, S. Cho, J.-L. Vivancos, Energy efficiency and thermal comfort in historic buildings: A review, Renew. Sustain. Energy Rev. 61 (2016) 70–85, https://doi.org/10.1016/j.rser.2016.03.018.

[27] UNESCO, Ferrara, City of the Renaissance, and its Po Delta, (1995). http://whc.unesco.org/en/list/733 (accessed January 9, 2019).

[28] M. Andreotti, M. Calzolari, P. Davoli, L. Dias Pereira, E. Lucchi, R. Malaguti, Design and construction of a new metering hot box for the in situ hygrothermal measurement in dynamic conditions of historic masonries, Energies. 13 (11) (2020) 2950, https://doi.org/10.3390/en13112950.

[29] P. Davoli, Complexity, information surplus and interdisciplinarity management. The Rehabilitation of Tassoni Estense Palace in Ferrara, in: JAIN K. et al. (Ed.), Conserv. Archit., AADI CENTRE, 2017: pp. 124–145. http://hdl.handle.net/11392/2359933.

[30] M. Andreotti, D. Bottino-Leone, M. Calzolari, P. Davoli, L. Dias Pereira, E. Lucchi, A. Troi, Applied research of the hygrothermal behaviour of an internally insulated historic wall without vapour barrier: in situ measurements and dynamic simulations, Energies. 13 (13) (2020) 3362, https://doi.org/10.3390/en13133362.

[31] O.M. Essenwanger, General Climatology 1C: Classification of Climates, Amesterdam (2001).

[32] Decreto del Presidente della Repubblica 26 agosto 1993, n. 412 - Regolamento recante norme per la progettazione, l'installazione, l'esercizio e la manutenzione degli impianti termici degli edifici ai fini del contenimento dei consumi di energia, Gazz. Uff. Della Repubb. Ital. 412 (1993) 155.

[33] HeLLo, HeLLo team has set-up the technical worktables!, (2019). https://hellomscaproject.eu/hello-team-has-set-up-the-technical-worktables/ (accessed January 15, 2020).

[34] M. Calzolari, P. Davoli, L. Dias Pereira, Internal building insulation systems for historic buildings: hygrothermal performance analysis, in: EDIZIONE ARCADIA RICERCHE Srl (Ed.), 36° Int. Conf. Eff. WATER Cult. Herit. Crit. Assessments Verif. Methods, Marghera Venezia/Venice, 2020: pp. 485–495. http://hdl.handle.net/11392/2435906.

[35] E. Lucchi L. Dias Pereira M. Andreotti R. Malaguti D. Cennamo M. Calzolari V. Frighi Development of a Compatible, Low Cost and High Accurate Conservation Remote Sensing Technology for the Hygrothermal Assessment of Historic Walls Electronics 8 6 643 10.3390/electronics8060643

[36] International Organization for Standardization (ISO), ISO 7730: 2005. Ergonomics of the thermal environment. Analytical determination and interpretation of thermal comfort using calculation of the PMV and PPD indices and local thermal comfort criteria, 2005.

[37] Ente Italiano di Normazione (UNI), UNI EN ISO 13788 Prestazione igrotermica dei componenti e degli elementi per edilizia - Temperatura superficiale interna per evitare l'umidita' superficiale critica e la condensazione interstiziale - Metodi di calcolo, 2013.

[38] International Organization for Standardization (ISO), ISO 17772-1: 2017. Energy performance of buildings — Indoor environmental quality — Part 1: Indoor environmental input parameters for the design and assessment of energy performance of buildings, 2017.

[39] Ente Italiano di Normazione (UNI), UNI EN 15026 Prestazione termoigrometrica dei componenti e degli elementi di edificio - Valutazione del trasferimento di umidità mediante una simulazione numerica, 2008.

[40] 3ENCULT, 3ENCULT Efficient Energy for EU Cultural Heritage, (n.d.). http://www.3encult.eu/en/project/welcome/default.html (accessed June 19, 2016).

[41] Fraunhofer IBP (Fraunhofer Institute for Building Physics), WUFI Pro-6.2 [Computer software], (2014).